Influence of buffer solution on structure and electrochemical properties of poly(3,4-ethylenedioxythiophene)/poly(styrenesulfonate) hydrogels

Anna Słoniewska[a,b,*], Mateusz Kasztelan[a,b], Sylwia Berbeć[a,b], Barbara Pałys[a,b]

[a] *Department of Chemistry, University of Warsaw, Pasteura 1, Warsaw, 02-093, Poland*
[b] *Chemical and Biological Research Center, University of Warsaw, Zwirki i Wigury 101, Warsaw, 02-089, Poland*

ARTICLE INFO

ABSTRACT

Numerous advantages of poly(3,4-ethylenedioxythiophene)/poly(styrenesulfonate) (PEDOT-PSS) hydrogel make this material appropriable for biosensors developing. Among many of them, it may be exploited as an immobilization matrix for binding bioreceptors. Porous 3-D structure facilitates high loading of the enzyme and extends surface area, what results in better biosensor performance and signal increase. High water content generates hydrophilic environment, thus biocompatibility is greatly enhanced. Citrate or phosphate buffers are typically used to provide optimal pH for the immobilized enzyme. The present work reports on the development of the PEDOT-PSS hydrogels synthesized in phosphate buffer or citrate buffer solutions at pH = 5 to verify the influence of the anion present in the polymerization environment on the molecular structure and electrochemical properties of the hydrogel. The water content in each hydrogel sample is estimated by weighting the swelled and dried samples and termogravimetric analysis. It is shown that PEDOT-PSS obtained in phosphate buffer solution comprises much more water than hydrogel synthesized in citrate buffer. This property is of great importance for the electrocatalytic properties of immobilized horseradish peroxidase (HRP). Wherefore, the PEDOT-PSS/HRP modified electrode has been used for the amperometric detection of H_2O_2 at pH = 6. The phosphate containing ph-PEDOT-PSS/HRP biosensor is characterized by a good linear relation with the concentrations of H_2O_2 with a linear range from 0.0088 to 0.15 mM and from 0.4 to 10 mM and a low detection limit of $9.4 \cdot 10^{-7}$ M and $4.5 \cdot 10^{-5}$ M (S/N = 3), respectively. While the citrate containing cit-PEDOT-PSS/HRP sensor shows worse analytical parameters - linear range from 0.05 to 0.25 mM and detection limit of $1 \cdot 10^{-5}$ M (S/N = 3).

1. Introduction

Electrically conductive hydrogels are novel class of materials founding application in many field including tissue engineering [1], electrode materials for supercapacitors [2] and sensor construction, where they can be used as both the sensing element or the support for enzymes [3,4] or aptamers [5].

The conductivity comes from the presence of redox centers [6] or electronically conducting polymers like polypyrrole, polyaniline or poly(3,4-ethylenedioxythiophene) (PEDOT) [7–9]. Hydrogels form stable layers on electrodes due to the presence of chemical crosslinks (tie-points, junctions) and/or physical crosslinks such as entanglements and crystallites or hydrogen bonds and electrostatic interactions. Great advantage of conductive hydrogels as support for enzymes is large content of water facilitating the diffusion of analyte within the layer. Water in the layer contributes also to the enzyme load and stability. The amount of water within the layer is affected also by several other factors, including buffer composition and presence of salts [10].

Among electronically conducting polymers PEDOT is distinguished by high conductivity coupled with high biocompability [11,12]. PEDOT-PSS forms a dispersion of particles in water at low concentrations (ca. 1%), which is available commercially. Some authors prepare composite hydrogels employing the PEDOT-PSS particles and non-conductive scaffold. For example hydrogel can be obtained by encapsulation of PEDOT-PSS solution into the gelatin methacryloyl (GelMA) using the photopolymerization technique [13] or by common dispersion of PEDOT-PSS (0–0.3 % (w/v)) in GelMA [14]. Bio-materials like alginate [15], agarose [16], biohybrid collagen – alginate [17] can be combined with PEDOT-PSS to form conductive hydrogel. Synthetic polymers like: polyacrylic acid (PAAc) [18], poly(ethylene glycol)-diacrylate (PEG-DA) [19], poly (N-acryloyl glycinamide-co-2- acryla-mide-2-methylpropanesulfonic) (PNAGA-PAMPS) [20], polyacrylamide

---

(PAAM) [21–23] and polyvinyl alcohol (PVA) [24] are used to produce the hydrogel containing PEDOT-PSS likewise.

PEDOT-PSS solution can be physically crosslinked by multivalent cations, including Mg^{2+}, Ca^{2+}, $Fe^{2+/3+}$ and $Ru(NH_3)_6^{2+/3+}$ to form a hydrogel [25,26]. Stable hydrogels of polyaniline were obtained by oxidation of the concentrated monomer (0.5 M) in PSS [27,28]. or phytic acid solution [29]. We apply similar method to obtain the PEDOT-PSS hydrogel by oxidation of EDOT in PSS solution at high concentration of the monomer.

Immobilized enzymes require stable pH of the environment. To ensure the optimal pH conditions citrate or phosphate buffers are typically used. The influence of the type of anion present in the polymerization bath on properties of PEDOT-PSS hydrogels was not studied up to our knowledge. In this contribution we investigate the PEDOT-PSS hydrogels synthesized in phosphate buffer (ph-PEDOT-PSS) and citrate buffer (cit-PEDOT-PSS) solution at pH = 6 to verify the influence of the polymerization environment on the molecular structure and electrochemical properties of the hydrogel. Next, the hydrogels were studied as possible supports for horseradish peroxidase (HRP). Spectroscopic and electrochemical methods were used to investigate the structure and properties of ph-PEDOT-PSS and cit-PEDOT-PSS hydrogels.

2. Experimental

2.1. Chemicals and reagents

Chemicals were commercial materials of the highest available grade, and they were used as received. 3,4-ethylenedioxythiophene (EDOT); poly(sodium 4-styrenesulphonate), PSSNa (average Mw 70,000, powder); ammonium persulfate, $H_8N_2O_8S_2$ (ACS reagent, 98 %); horseradish peroxidase, HRP (type VI-A lyophilized powder; E.C.1.11.1.7, 250–330 units per mg); 5% Nafion-117 solution were obtained from Sigma Aldrich. Monosodium phosphate, disodium phosphate, sodium citrate, citric acid and 30 % hydrogen peroxide were obtained from Avantor Performance Materials Poland S.A. Phosphate buffer solution with pH = 6.0 and citrate buffer solution with pH = 6.0 were prepared using distilled (18.2 mΩ Millipore Milli-Q) water.

2.2. Electrochemical experiments

All electrochemical experiments were performed in a conventional three-electrode cell using PGSTAT204 potentiostat/galvanostat from MetrohmAutolab BV, operated by the NOVA 1.10 software. A glassy carbon disk electrode (geometric area, 0.071 cm²) was used as the working electrode. A platinum wire served as the counter electrode. All potentials were measured vs. Ag|AgCl (3 mol·dm⁻³KCl) reference electrode. Before modification, a working electrode was activated by polishing with aqueous alumina slurries (grain size 3 μm). The sweep rate (v) was set to 10 mV/s in the cyclic voltammetry experiments.

All electrochemical experiments were carried out in aqueous solution at pH = 6 at temperature equal to 23 °C. The 0.1 M phosphate buffer solution was used for ph-PEDOT-PSS and the 0.1 M citrate buffer solution was used for cit-PEDOT-PSS samples. The pH of buffer solutions was verified by the pH-meter (ELMETRON, CPO-401).

2.3. Infrared spectra

Infrared spectra were recorded using the Nicolet iS50 FT-IR spectrophotometer from Thermo Scientific. Due to the hydrogel nature of PEDOT–PSS composite IR experiments were carried out using the smart iTR attenuated total reflection accessory with the diamond crystal. The samples were cast directly on the top of the diamond crystal. The spectral resolution was 4 cm⁻¹, and typically, 256 scans were averaged for a single spectrum.

2.4. Resonance Raman spectra

The Raman experiments were carried out using a DXR Raman spectrometer (Thermo Scientific). The instrument was operated using a 633-nm excitation line. For typical experiments, the spectral resolution was equal to 1 cm⁻¹. The 50/0.50 objective was used. In the configuration used, the signal was collected from the 1-μm³ spot. The laser beam was focused on top of the layer to minimize the contribution of the GCE support to the spectra.

2.5. Scanning electron microscopy

The morphology of hydrogels was investigated by Merlin field emission scanning electron microscope system (Zeiss, Germany). Hydrogel layer was deposited on the gold surface. The sample was left for two hours in air atmosphere for drying before the experiment.

2.6. Thermogravimetric analysis

Thermogravimetry data were collected with TGA Q50 (TA Instruments). The temperature was scanned with the rate: 20 °C/min. The sample was kept at the final temperature (150 °C) for 10 min to ensure the total evaporation of water.

2.7. Samples preparation

PEDOT–PSS hydrogel was prepared according to the procedure described by Dai and Jia for polyaniline – PSS hydrogels with some modification [27]. The concentrations of reagent we used to obtain the mechanically stable hydrogel were equal to 0.5 mol·dm⁻³ for EDOT, ammonium persulfate and PSS. The use of PSS enhances the solubility of EDOT in aqueous solution, which itself is unable to form a film [30]. The reaction was carried out in the buffer solutions - in the phosphate buffer, pH = 6.0 (receiving ph-PEDOT-PSS), and in the citrate buffer, pH = 6.0 (receiving cit-PEDOT-PSS). The reaction was carried out for 12 h.

Received hydrogel was deposited on GCE, rinsed with distilled water and left for drying in air for 2 h. After drying, 12 μl of the HRP solution (20 mg/ml) in phosphate or citrate buffer at pH = 6 was poured onto the electrode. The electrode was left to dry in a humidified atmosphere at 4 ⁰C for at least 2 h. The electrode was rinsed with Milli-Q water. Subsequently, 2 μl of the 5% Nafion 117-ethanol solution (1:10) was dropped on the electrode [11,56,58,59]. The electrode was left in air for 10 min and then transferred into the electrochemical cell.

2.8. Water content by weighting

Water content of the hydrogels is the weight percentage of water in saturated hydrogels and it was evaluated from the following equation:

$$\text{Water content} = (W_s - W_d)/W_s \cdot 100 \% \qquad (1)$$

where Ws and Wd are the fully swollen and dry weight of each sample, respectively. Hydrogels were dried in the oven in 50⁰C overnight. The samples were weighed on the analytical balance. Five samples of each hydrogel were studied. The swelling degree values are average of the five measurements. The error was calculated as the standard deviation.

3. Results and discussion

3.1. Morphology of the hydrogels

Polymerization of EDOT in the presence of the PSS sodium salt (PSSNa) (each with a concentration of 0.5 mol·dm⁻³) in the phosphate buffer environment results in a hydrogel with a three-dimensional, porous structure (Fig. 1).

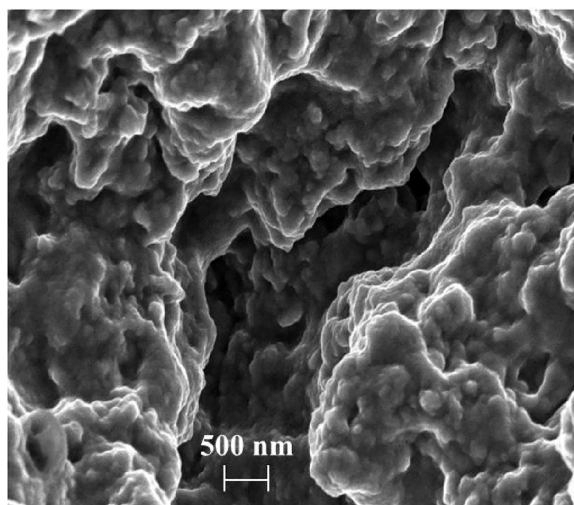**Fig. 1.** SEM image of PEDOT-PSS hydrogel synthesized in phosphate buffer.

Table 1
Comparison of water content in hydrogels.

Hydrogel sample	Oven drying at 50 °C	Thermogravimetric analysis
ph-PEDOT-PSS	69 % (+/- 0.2) wt-%	73 % (+/- 0.1) wt-%
cit-PEDOT-PSS	41 %(+/- 0.2) wt-%	33 % (+/- 0.1) wt-%

content comparing to ph-PEDOT-PSS hydrogel. The water content values obtained by weighting and the termogravimetry experiments are collected in the Table 1. The accuracy of both measurements was estimated from the standard deviation of the results obtained for five samples.

To rationalize the differences in the water content the dissociation of phosphate and citrate anions has to be considered. According to phosphoric acid speciation and citric acid speciation mostly $H_2PO_4^-$ (pK_{a2} = 7.21, ionic charge: -1) and AH^{2-} (pK_{a3} = 6.39, ionic charge: -2) (where AH_3 is citric acid) ions are present in the used buffer solutions. Due to the smaller size of phosphate ions and probably also a smaller solvation shell they show higher mobility and can exchange freely in the system during polymerization, and then the catalytic reaction. The viscosity B-coefficients could be more quantitative measure of the anion properties [31]. The B-coefficients are experimental parameters quantifying the influences of solutes species on the viscosity of the solution. They are known to provide information concerning the solvation of the ions and their effects on the structure of the solvent in the near environment of the solute ions (or molecules). The positive value of the B-coefficient indicates the increase of viscosity. The B-coefficient of aqueous inorganic $H_2PO_4^-$ ion is 0.340 dm^3/mol at 25 °C [59]. The analogic B-coefficient value for the monovalent citrate ion (AH_2^-) equals to 0.658 dm^3/mol [32]. Both anions increase thus the viscosity of the solution, but the effect of citrates is bigger comparing to phosphates, what contributes probably to the difference in swelling of ph-PEDOT-PSS and cit-PEDOT-PSS by water.

The differences in both ions can be caused also because of their position in Hofmeister series [33]. Citrate ions lay in the series on the left, what means that they can be classified as kosmotropes – or "water structure making" anions. The $H_2PO_4^-$ ions are in the middle of the series –being on the border between kosmotropic and chaotropic anions. The hydration shell of kosmotropic ions is ordered and the density of water forming the hydration sphere is higher comparing to bulk of the solution [61]. Anions with such dense hydration sphere are not diffusing into hydrophobic polymer layers. The hydrophobicity of PEDOT probably hampers penetration of citrates into PEDOT-PSS system.

Water present in hydrogel acts like a plasticizer – intermolecular interactions between polymer chains diminish what yields better polymer chains mobility. Thanks to this feature, swelled hydrogels are more permeable to small molecules, which allows, among others, for more efficient diffusion of the analyte within the hydrogel matrix. Thus, it appears that ph-PEDOT-PSS is a more appropriate material for the construction of biosensors, because it contains more water.

3.2. Water content

Using the Eq. (1), it is possible to determine the water content in each hydrogel. Typically, the water contents of ph-PEDOT-PSS and cit-PEDOT-PSS are 69 (+/- 0.2) wt-% and 41 (+/-0.2) wt-%, respectively. Such weighting of swelled and dried samples indicates significant differences in the water content. To verify this observation we carried out the termogravimetry experiments. The typical results are shown in Fig. 2. As seen for the ph-PEDOT-PSS hydrogel, the mass decreases to nearly 27 % of the initial value at the temperature equal to 150 °C. The sample was kept at 150 °C to ensure the complete water evaporation. No further mass decrease was observed.

The mass of the cit-PEDOT-PSS diminished to approximately 67 % of the initial value as illustrated by Fig. 2, confirming the smaller water
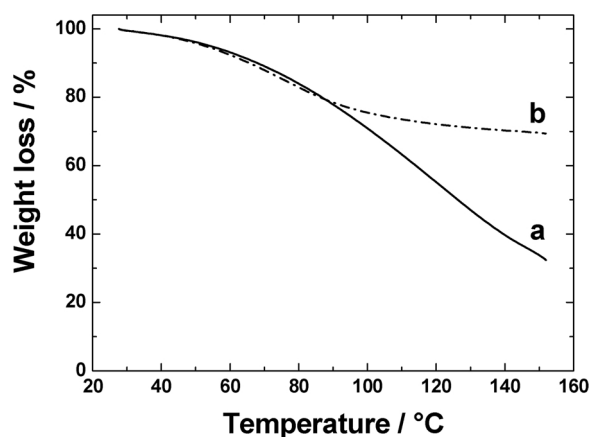
3.3. Infrared and Raman spectra

The spectroscopic properties of PEDOT-PSS hydrogels were examined using infrared spectroscopy and Raman spectroscopy.

ATR-FTIR spectroscopy was used to qualitative investigation of obtained polymeric composites. Fig. 3 compares typical infrared spectra of the PEDOT-PSS hydrogels prepared in two different buffer solutions. Hydrogels layers of similar thickness were deposited on the ATR diamond prism. The spectra were recorded after drying using the infrared microscope working in the attenuated total reflection mode. Considering the presence of water in the examined samples, it is not surprising that there are characteristic bands from this solvent on the spectra, at 3384 cm^{-1} from the stretching vibrations of $-OH$ group in
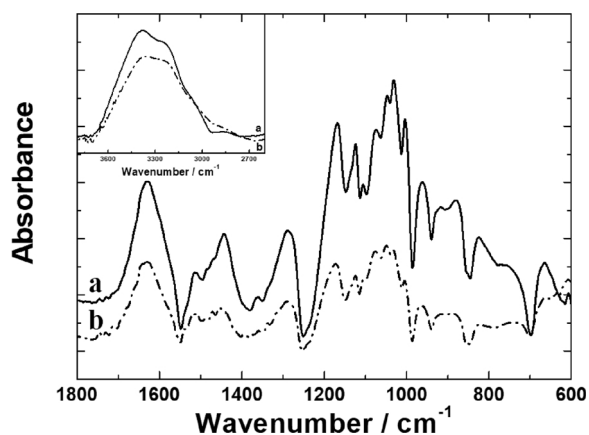

Fig. 2. Thermogravimetric curves of: a) ph-PEDOT-PSS hydrogel, b) cit-PEDOT-PSS hydrogel.

Fig. 3. ATR-FTIR spectra of PEDOT-PSS hydrogel prepared in (a) phosphate buffer, (b) citrate buffer.

the free and absorbed water and at $1630 \, cm^{-1}$ from the H−O−H bending vibration of the residual water [34]. On the basis of the intensity ratio of these bands it can be concluded that the ph-PEDOT-PSS hydrogel contains more water in its structure than cit-PEDOT-PSS hydrogel. Water filling the space of the polymer skeleton is desirable because it facilitates the transport of small molecules throughout the entire volume of the structure. Therefore, the ph-PEDOT-PSS hydrogel should exhibit better results as a biosensor compared to cit-PEDOT-PSS, as shown by further results with H_2O_2. The presented spectra of both samples also contain PSS characteristic bands, which is applied as a co-solvent and dopant, especially bands derived from -SO_3 groups (1169, 1125, 1033 and $1005 \, cm^{-1}$) [35]. In addition, band at $1630 \, cm^{-1}$ overlapping one of the water bands is assignable to the C═C stretching vibrations of the aromatic PSS ring. The band around $1445 \, cm^{-1}$ assigns to the stretching of C═C in the thiophene ring. For the cit-PEDOT-PSS hydrogel this band is smaller and shifted towards higher wavelengths ($1457 \, cm^{-1}$). The band at $1290 \, cm^{-1}$ indicates the stretching vibrations of the C−O−C bond in the ethylene dioxy(alkylenedioxy) group [36], and the bands at 1048 and $1169 \, cm^{-1}$ are corresponding to the symmetric and asymmetric stretching of S═O. The bands at 962, 881 and $665 \, cm^{-1}$ are derived from the deformation vibrations of the C–S group in the polymer structure, and they are the fingerprint absorption of PEDOT [37]. Whereas the band at $1747 \, cm^{-1}$ indicates the PEDOT-doped state [38]. These data demonstrate the existence of PEDOT-PSS. Because synthesis of the ph-PEDOT-PSS hydrogel has been carried out in the phosphate environment the absorption around

$1074 \, cm^{-1}$ indicates presence of P-O- species in H_2PO_4- and HPO_4^{2-} ions in the hydrogel [39,40]. This figure confirms also the presence of the citrate ions present in the cit-PEDOT-PSS hydrogel synthesis environment. The low intensity band observed at $1473 \, cm^{-1}$ is assigned to the symmetrical stretching of the citrate ion carboxylates [41,42]. While the band of asymmetric vibrations of COO- ($\sim 1586 \, cm^{-1}$) is invisible, probably covered by the strong band from the H−O−H bending vibration of the residual water located at $1630 \, cm^{-1}$. The intensities of typical bands for PSS and phosphate/citrate ions were compared. Their ratios are as follows: PSS:phosphate = 0.99 ≈ 1 and PSS:citrate = 2.21. It thus proves that phosphate ions penetrate hydrogel matrix more efficiently than citrate ions. Moreover, it is very probable that the small phosphate ions can be effectively transported through the hydrogel what seems hindered in case of citrate ions. Besides, transport of such large anions would give exceedingly low ionic conductivities, which is not eligible when using such hydrogel in electrochemical biosensors. Furthermore, due to the fact that phosphate acid is stronger than citric acid, water is more strongly attracted in ph-PEDOT-PSS hydrogel, which is consistent with the calculations of weight percentage of water in saturated hydrogels. While synthesis environment does not change the PEDOT to PSS ratio (in both samples amounts to 0.5).

Raman spectroscopy was used to determine the molecular structure of PEDOT-PSS hydrogels. The spectra of as-prepared PEDOT–PSS layers are shown in Fig. 4A. Both, for ph-PEDOT-PSS (Fig. 4a) and for cit-PEDOT-PSS (Fig. 4b) they are very similar. The highest intensity shows bands derived from PEDOT. The central point of the Raman spectrum is the band from the symmetric stretching vibrations of the C═C group in the polymer ring, which can be observed at $1422 \, cm^{-1}$; this band is characteristic of polythiophenes. Its position depends on the length of the coupling (number of double bonds in the chain) and coincides with the literature data ($1419 \, cm^{-1}$ [43]). The lack of bands at 682 and $655 \, cm^{-1}$, associated with defects in the polymer chain, indicates a planar structure of the sample [44,45]. This confirms the presence of weak bands at 1130 and $1096 \, cm^{-1}$ characteristic of deformed C−C bonds between the rings in the polymer chain [46]. This proves that the obtained system is highly conjugated. The next three very important bands are also visible at 1529, 1359 and $1248 \, cm^{-1}$ indicating, respectively, asymmetric C−C bond stretching vibrations, and at the smallest wavenumber C−C stretching vibrations within the ring.

Fig. 4B shows spectra from 1200 to $1700 \, cm^{-1}$, where the strongest change in both spectra is observed. It refers to the band located at $1496 \, cm^{-1}$ corresponding to the asymmetric stretching vibration of C═C on the five-member ring of PEDOT [47,48]. The difference in the intensity of this band for both samples indicates different conformation
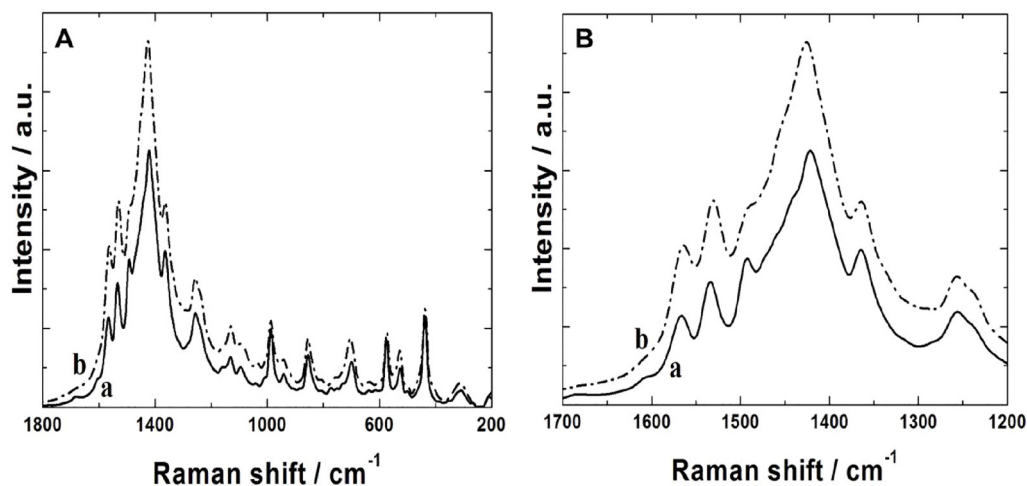

Fig. 4. A) Raman spectra of PEDOT-PSS hydrogel prepared in (a) phosphate buffer, (b) citrate buffer. Excitation line: 633 nm. B) Bands in the range: 1700–1200 cm^{-1}.

Fig. 5. Cyclic voltammograms of: a) ph-PEDOT–PSS hydrogel and b) cit-PEDOT-PSS in the buffer solutions pH = 6, scan rates: 10 mV/s.

of the polymer chains depending on the ions present in the reaction environment. This has been proven for other conducting polymers that the kind of anions influences the morphology of polymer samples as well as their oxidation and conformation states. For instance, in presence of ClO_4^- anions PANI nanotubules with planar conformation are obtained, while in Cl^- anions polymer nanostructures with twisted conformation are formed [49]. Also the structure of polypyrrole undergoes rearrangement of polymer chain packing depending on the type of anions present in the environment [50].

3.4. Cyclic voltammetry

Fig. 5. Cyclic voltammograms of: a) ph-PEDOT–PSS hydrogel and b) cit-PEDOT-PSS in the buffer solutions pH = 6, scan rates: 10 mV/s.

The electroactivity of ph-PEDOT-PSS and cit-PEDOT-PSS was studied in aqueous buffer solutions at pH = 6. Typical results are presented in Fig. 5. As visible both PEDOT-PSS layers are electroactive in aqueous solutions. The shapes of cyclic voltammetry responses are similar to the results reported for EDOT electropolymerized in presence of PSS [51] or sodium dodecyl sulfate [52]. The observed redox couple corresponds to the oxidation of the neutral PEDOT to oxidized - conductive PEDOT and reduction to the neutral polymer in the back scan. Following references [51] and [52] the reaction is described by the equation:

$$EDOT_n^0 \cdot SS^- \cdot C^+ - \bar{e} - C^+ \leftrightarrow EDOT_n^+ \cdot SS^-$$

neutral   conductive   (1)

where $EDOT_n^0$ is the neutral monomeric unit of PEDOT, $EDOT_n^+$ is the

Fig. 7. Calibrations plot for the amperometric response of ph-PEDOT-PSS/HRP with the successive addition of H_2O_2. Inset: response for lower concentration of H_2O_2 (0.0088 - 0.15 mM).

oxidized unit, the SS^- stands for the sulfate group of PSS and C^+ is cation from the supporting electrolyte.

The charge formed by the oxidation can be compensated by expulsion of cations from the layer as in Eq. (1) or incorporation of anions from the supporting electrolyte.

As illustrated in Fig. 5, the current values observed for ph-PEDOT-PSS are always higher comparing to cit-PEDOT-PSS. Such difference can be rationalized by various swelling properties of the two hydrogels, which in turn causes differences in diffusion of ions necessary for the charge compensation. Water filling the spaces of the polymer scaffold, facilitates the transport of small particles in the entire volume of the structure. Thus, ph-PEDOT-PSS hydrogel that contains more water in its structure (69 wt-% compared to cit-PEDOT-PSS with 41 wt-% of water) shows higher electroactivity.

3.5. Amperometric detection of H_2O_2

The amperometric responses of PEDOT-PSS were studied at +0.20 V vs Ag/AgCl in a deoxygenated solution. The effect of successive additions of H_2O_2 on the amperograms of HRP physically adsorbed on ph-PEDOT-PSS and cit-PEDOT-PSS hydrogels are shown in Fig. 6. The control experiments were carried out for the hydrogels without the immobilized enzyme (Figure S1). The responses to H_2O_2 of the layers without the enzyme are observed at thousand times higher concentrations of H_2O_2 comparing to the layers with HRP.

The current response of the physically adsorbed enzyme is visible,

Fig. 6. Amperometric response of HRP physically adsorbed on: A) ph-PEDOT-PSS (H_2O_2 addition: the smallest - 0.0088 mM, up to 0.88 mM), B) cit-PEDOT-PSS (H_2O_2 addition: up to 0.044 mM).

Table 2

Comparison of the sensitivities of various H_2O_2 sensors based on PEDOT composites.

Composite	Sensitivity	Linear range	Detection limit (M)	References
ITO/PEDOT-PSS/HRP	0.544 µA/mM	up to 1 mM	–	[54]
PEDOT-PSS/GOD/HRP	20.5 µA/mM	0.59 – 1.44 mM	$2.7 \cdot 10^{-4}$	[55]
PEDOT/P4VPy/Os/HRP	130 µA/mM	0 – 30 µM	–	[9]
PEDOT-PSS-MDB	353.9 µA/mM	5 – 120 µM	$1.0 \cdot 10^{-7}$	[56]
PEDOT/PB/PPyBA/HRP	1.15 µA/mM	100 – 700 µM	$3.0 \cdot 10^{-5}$	[57]
HRP/PEDOT-PSS/Au	63 µA/mM	0.2 – 380 µM	$1.0 \cdot 10^{-7}$	[58]
HRP/AgNPs/PEDOT-PSS/GCE	21300 µA/mM	0.05 – 20 µM	$2.0 \cdot 10^{-8}$	[59]
PEDOT-PSS/rGO/AuNPs	677 µA/mM	5 – 400 µM	$8.0 \cdot 10^{-8}$	[60]
HRP/GO/Nafion/GCE	–	1 – 1000 µM	$1.0 \cdot 10^{-7}$	[61]
Nafion/HRP/graphene/GC	–	0.33 – 13 µM	$1.1 \cdot 10^{-7}$	[62]
ph-PEDOT-PSS/HRP	155 µA/mM 3.5 µA/mM	0.0088 – 0.15 mM 0.4 – 10 mM	$9.4 \cdot 10^{-7}$ $4.5 \cdot 10^{-5}$	this work
cit-PEDOT-PSS/HRP	49 µA/mM	0.05 – 0.25 mM	$1 \cdot 10^{-5}$	this work

P4VPy - Poly(4-vinylpyridine), PB - Prussian Blue, PPyBA - 4(pyrrole-1-yl)-benzoicacid, MDB - Meldola Blue, GOD - GlucoseOxidase, AgNPs – silvernanoparticles, AuNPs – goldnanoparticles.

as ilustrated in Fig. 6A. Unfortunately, current stabilization takes time, what indicates weak diffusion. Therefore, the hydrogel has a problem with reaching a steady state between addition of H_2O_2, but the system reacts to the addition of the studied analyte in a wide range of concentrations. Using cit-PEDOT-PSS as a matrix for HRP, the H_2O_2 diffusion is even worse, the system stops responding to further H_2O_2 additions in a short time (Fig. 6B).

The sensitivity of the ph-PEDOT-PSS/HRP system was 0.0035 $mA \cdot cm^{-2} mM^{-1}$ (in the range from 0.4 mM to 10 mM), based on the slope of the current concentration dependence (Fig. 7). The detection limit of this biosensor was estimated to be $4.52 \cdot 10^{-5}$ M (i.e., 3 the S/N ratio [58,59]). For lower concentrations, up to 0.4 mM, the sensitivity is much higher and reaches 0.155 $mA \cdot cm^{-2} mM^{-1}$, whereas the detection limit is also higher and amounts to $9.40 \cdot 10^{-7}$ M (i.e., 3 the S/N ratio). The cit-PEDOT-PSS/HRP system is characterized by worse parameters. In the 0.05-0.25 mM range, the sensor sensitivity is 0.049 $mA \cdot cm^{-2} mM^{-1}$ and the detection limit is $1 \cdot 10^{-5}$ M. Unfortunately, for higher concentration of H_2O_2, up to 0.25 mM, we have observed non-linear amperometric responses from cit-PEDOT-PSS/HRP system (Fig. 6B).

Table 2 shows comparison of the sensitivities of various H_2O_2 sensors based on PEDOT composites.

PEDOT layers has been studied as possible supports for HRP either as pure films or combined with redox mediators or metallic or carbon nanostructures. As illustrated in the Table 2 HRP immobilized in homogenous PEDOT layers shows lower sensitivity comparing to HRP immobilized in PEDOT layers with a redox mediator (like MDB, PB or Os complexes). PEDOT composed with osmium complexes or MDB mediator show similar sensitivity to the PEDOT-PSS hydrogels described in this work. Sensors involving the composites with reduced graphene oxide or metal nanoparticles show similar or better sensitivity, though graphene oxide and noble metal nanoparticles show intrinsic catalytic properties towards the H_2O_2 reduction [53].

4. Conclusions

In this work, we reported PEDOT-PSS hydrogels synthesized in phosphate and citrate buffer solutions. According to our results, presence of different ion strongly influence the water content in hydrogel. Almost 30 % higher water amount in ph-PEDOT:PSS comparing to cit-PEDOT:PSS translates directly into better biosensor performance. The differences can rationalized taking into account viscosity B-coefficient of citrates and phosphates, as well as the Hofmeister effect. Water provides more efficient diffusion of the analyte within the hydrogel matrix, what makes hydrogels appropriate materials for biosensor designing. Additionally, hydrogels possess large surface area available for enzyme binding. Both of mentioned factors enhance electrocatalytic

activity of adsorbed HRP. We obtained H_2O_2 sensor with 0.0035 $mA \cdot cm^{-2} mM^{-1}$ sensitivity and $4.13 \cdot 10^{-5}$ M limit of detection. Based on available literature, the polymerization of EDOT is usually performed in acetonitrile or acid solutions, whereas optimum pH value for HRP is between 6 and 8. Therefore, we obtained PEDOT-PSS hydrogel in buffer solutions at pH = 6 to avoid the decrease of enzyme activity. PEDOT-PSS hydrogels synthesized in phosphate buffer solution are promising material for further modification with metal nanoparticles to receive biosensors with better sensitivity and lower limit of detection.

5. Author statement

Anna Słoniewska: corresponding author, writing the text, performing part of experiments (enzyme immobilization and activity, Raman spectra); Mateusz Kasztelan experiments - thermogravimetry, Sylwia Berbeć experiments – cyclic voltammetry, Barbara Pałys discussion of the results with corresponding author, help with interpretation, part of experiments (spectroscopy).

Declaration of Competing Interest

The authors declare that they have no known competing financial interests or personal relationships that could have appeared to influence the work reported in this paper.

Appendix A. Supplementary data

Supplementary material related to this article can be found, in the online version, at doi:https://doi.org/10.1016/j.synthmet.2020.116363.

References

[1] T. Distler, A.R. Boccaccini, 3D printing of electrically conductive hydrogels for tissue engineering and biosensors – a review, Acta Biomater. 101 (2020) 1–13.

[2] H. Li, J.J. Yuan, L. Zha, L.Y. Wang, H.Q. Chen, J.F. Che, Soft conducting polymer hydrogels in situ doped by sulfonated graphene quantum dots for enhanced electrochemical activity, J Mater Sci-Mater El (2019), https://doi.org/10.1007/s10854-019-02739-2.

[3] M. Ikeda, R. Ochi, I. Hamachi, Supramolecular hydrogel-based protein and chemosensor array, Lab Chip 10 (2010) 3325–3334.

[4] A. Słoniewska, B. Pałys, Supramolecular polyaniline hydrogel as a support for urease, Electrochim. Acta 126 (2014) 90–97.

[5] X.Y. Wang, F.X. Gao, Y.Y. Gong, G.T. Liu, Y. Zhang, C.F. Ding, Electrochemical aptasensor based on conductive supramolecular polymer hydrogels for thrombin detection with high selectivity, Talanta 205 (2019) 120140.

[6] A. Heller, Electron-conducting redox hydrogels: design, characteristics and synthesis, Curr. Opin. Chem. Biol. 19 (2006) 664–672.

[7] A. Guiseppi-Elie, Electroconductive hydrogels: synthesis, characterization and biomedical applications, Biomaterials 31 (2010) 2701–2716.

[8] J. Stejskal, Conducting polymer hydrogels, Chem. Pap. 71 (2017) 269–291.

[9] P. Åsberg, O. Inganäs, Hydrogels of a conducting polymers as a 3-D enzyme electrode, Biosens. Bioelectron. 13 (2003) 199–207.

[10] R.A. Siegel, B.A. Firestone, pH-dependent equilibrium swelling properties of hydrophobic polyelectrolyte copolymer gels, Macromolecules 21 (1988) 3254–3259.

[11] G. Kaur, R. Adhikari, P. Cass, M. Bown, P. Gunatillake, Electrically conductive polymers and composites for biomedical applications, RSC Adv. 5 (2015) 37553–37567.

[12] D. Gao, K. Parida, P.S. Lee, Adv. Funct. Mater. (2019) art. number 1907184.

[13] S. Oktay, N. Alemdar, Electrically controlled release of 5-fluorouracil from conductive gelatin methacryloyl-based hydrogels, J. Appl. Polym. Sci. 136 (2019) 46914–46921.

[14] A.R. Spencer, A. Primbetova, A.N. Koppes, R.A. Koppes, H. Fenniri, N. Annabi, Electroconductive gelatin Methacryloyl-PEDOT:PSS composite hydrogels: design, synthesis, and properties, ACS Biomater. Sci. Eng. 4 (2018) 1558–1567.

[15] K. Wang, L. Tian, T. Wang, Z. Zhang, X. Gao, L. Wu, B. Fu, X. Liu, Electrodeposition of alginate with PEDOT/PSS coated MWCNTs to make an interpenetrating conducting hydrogel for neural interface, Compos. Interface. 26 (2019) 27–40.

[16] Y. Ko, J. Kim, H.Y. Jeong, G. Kwon, D. Kim, M. Ku, J. Yang, Y. Yamauchi, H.-Y. Kim, C. Lee, J. You, Antibacterial poly (3,4-ethylenedioxythiophene):poly(styrene-sulfonate)/ agarose nanocomposite hydrogels with thermo-processability and self-healing, Carbohyd. Polym. 203 (2019) 26–34.

[17] K. Roshanbinfar, L. Vogt, B. Greber, S. Diecke, A.R. Boccaccini, T. Scheibel, F.B. Engel, Electroconductive biohybrid hydrogel for enhanced maturation and beating properties of engineered cardiac tissues, Adv. Funct. Mater. 28 (2018) 1803951–1803961.

[18] V.R. Feig, M. Helen, Z. Bao Lee, Mechanically tunable conductive interpenetrating network hydrogels that mimic the elastic moduli of biological tissue, Nat. Commun. 9 (2018) 2740–2748.

[19] R.K. Pal, E.E. Turner, B.H. Chalfant, V.K. Yadavalli, Mechanically robust, photo-patternable conductive hydrogel composites, React. Funct. Polym. 120 (2017) 66–73.

[20] Q. Wu, J. Wei, B. Xu, X. Liu, H. Wang, W. Wang, Q. Wang, W. Liu, A robust, highly stretchable supramolecular polymer conductive hydrogel with self-healability and thermo-processability, Sci. Rep-UK 7 (2017) 41566–41576.

[21] B.C. Lim, B.S. Singu, S.E. Hong, Y.H. Na, K.R. Yoon, Synthesis and characterization nanocomposite of polyacrylamide-rGO-Ag-PEDOT/PSS hydrogels by photo polymerization method, Polym. Adv. Technol. 27 (2016) 366–373.

[22] T. Dai, X. Qing, H. Zhou, C. Shen, J. Wang, Y. Lu, Mechanically strong conducting hydrogels with special double-network structure, Synth. Met. 160 (2010) 791–796.

[23] F.A. Aouada, M.R. Guilherme, G.M. Campese, E.M. Girotto, A.F. Rubira, E.C. Muniz, Electrochemical and mechanical properties of hydrogels based on conductive poly (3,4-ethylene dioxythiophene)/poly(styrenesulfonate) and PAAm, Polym. Test. 25 (2006) 158–165.

[24] X. Zhang, J. Liu, B. Xu, Y. Su, Y. Luo, Ultralight conducting polymer/carbon nanotube composite aerogels, Carbon 49 (2011) 1884–1893.

[25] M. Vázquez, P. Danielsson, J. Bobacka, A. Lewenstam, A. Ivaska, Solution-cast films of poly(3,4-ethylenedioxythiophene) as ion-to-electron transducers in all-solid-state ion-selective electrodes, Sens. Actuators B Chem. 97 (2004) 182–189.

[26] C.H.L. Weijtens, V. van Elsbergen, M.M. de Kok, S.H.P.M. de Winter, Effect of the alkali metal content on the electronic properties of PEDOT:PSS, Org. Electron. 6 (2005) 97–104.

[27] A. Jabłońska, B. Pałys, Effect of the polymerization bath on structure and electrochemical properties of polyaniline-poly(styrene sulfonate) hydrogels, J. Electroanal. Chem. 784 (2017) 115–123.

[28] T. Dai, Y. Jia, Supramolecular hydrogels of polyaniline-poly(styrene sulfonate) prepared in concentrated solutions, Polymer 52 (2011) 2550–2558.

[29] L. Pan, G. Yu, D. Zhai, H.R. Lee, W. Zhao, N. Liu, H. Wang, B.C.-K. Tee, Y. Shi, Y. Cui, Z. Bao, Hierarchical nanostructured conducting polymer hydrogel with high electrochemical activity, PNAS 109 (2012) 9287–9292.

[30] B. Fan, X. Mei, J. Ouyang, Significant conductivity enhancement of conductive poly (3,4-ethylenedioxythiophene): poly(styrenesulfonate) films by adding anionic surfactants into polymer solution, Macromolecules 41 (2008) 5971–5973.

[31] H. Donald, B. Jenkins, Y. Marcus, Viscosity S-Coefficients of ions in solution, Chem. Rev. 95 (1995) 2695–2724.

[32] M.L. Parmar, R.K. Awasthi, M.K. Guleria, A study on viscosities of citric acid and tartaric acid in water and binary aqueousmixtures of ethanol at different temperatures, Indian J. Chem. 43A (2004) 41–44.

[33] Y. Zhang, P.S. Cremer, Chemistry of Hofmeister Anions and osmolytes, Annu. Rev. Phys. Chem. 61 (2010) 63–83.

[34] P. Sen, A. De, Electrochemical performances of poly(3,4-ethylenedioxythiophene)–NiFe2O4 nanocomposite as electrode for supercapacitor, Electrochim. Acta 55 (2010) 4677–4684.

[35] L. Chen, C. Yuan, H. Dou, B. Gao, S. Chen, X. Zhang, Synthesis and electrochemical capacitance of core–shell poly (3,4-ethylenedioxythiophene)/poly (sodium 4-styrenesulfonate)-modified multiwalled carbon nanotube nanocomposites, Electrochim. Acta 54 (2009) 2335–2341.

[36] C. Kvarnstrom, H. Neugebauer, S. Blomquist, H.J. Ahonen, J. Kankare, A. Ivaska, N.S. Sariciftci, In situ FTIR spectroelectrochemical characterization of poly(3,4-ethylenedioxythiophene) films, Synth. Met. 101 (1999) 66.

[37] J.W. Choi, M.G. Han, S.Y. Kim, S.G. Oh, S.S. Im, Poly(3,4-ethylenedioxythiophene) nanoparticles prepared in aqueous DBSA solutions, Synth. Met. 141 (2004) 293–299.

[38] S.V. Selvaganesh, J. Mathiyarasu, K.L.N. Phani, V. Yegnaraman, Chemical synthesis of PEDOT–Au nanocomposite, Nanoscale Res. Lett. 2 (2007) 546–549.

[39] M. Klahn, G. Mathias, C. Kotting, M. Nonella, J. Schlitter, K. Gerwert, P. Tavan, IR spectra of phosphate ions in aqueous solution: predictions of a DFT/MM approach compared with observations, J. Phys. Chem. A 108 (2004) 6186–6194.

[40] G. Socrates, Infrared Raman Characteristic Group Frequencies, John Wiley& Sons Ltd, 2011, pp. 636–637.

[41] J.C. Mohan, G. Praveen, K.P. Chennazhi, R. Jayakumar, S.V. Nair, Functionalised gold nanoparticles for selective induction of in vitro apoptosis among human cancer cell lines, J. Exp. Nanosci. 8 (2013) 32–45.

[42] A. Sobczak-Kupiec, D. Malina, M. Zimowska, Z. Wzorek, Characterization of gold nanoparticles for various medical application, Dig. J. Nanomater. Bios. 6 (2011) 803–808.

[43] J.L. Duvail, P. Retho, S. Garreau, G. Louarna, C. Godon, S. Demoustier-Champagne, Transport and vibrational properties of poly(3,4-ethylenedioxythiophene) nanofibers, Synth. Met. 131 (2002) 123–128.

[44] J.L. Sauvajol, D. Chenouni, J.P. Lère-Porte, C. Chorro, B. Moukala, J. Petrissans, Resonant Raman spectra and photoluminescence in polythiophene, Synth. Met. 38 (1990) 1–12.

[45] J. Bukowska, K. Jackowska, In situ Raman studies of polypyrrole and polythiophene films on Pt electrodes, Synth. Met. 35 (1990) 143–150.

[46] E.A. Bazzaoui, S. Aeiyach, P.C. Lacaze, Electropolymerization of bithiophene on Pt and Fe electrodes in an aqueous sodium dodecylsulfate (SDS) micellar medium, Synth. Met. 83 (1996) 159–165.

[47] S. Garreau, G. Louarn, J.P. Buisson, G. Froyer, S. Lefrant, In Situ Spectroelectrochemical Raman Studies of Poly(3,4-ethylenedioxythiophene) (PEDT), Macromolecules 32 (1999) 6807–6812.

[48] M. Łapkowski, A. Proń, Electrochemical oxidation of poly (3,4-ethylenedioxythiophene) — "in situ" conductivity and spectroscopic investigations, Synth. Met. 110 (2000) 79–83.

[49] M. Tagowska, B. Pałys, K. Jackowska, Polyaniline nanotubules—anion effect on conformation and oxidation state of polyaniline studied by Raman spectroscopy, Synth. Met. 142 (2004) 223–229.

[50] Q. Pei, R. Qian, Protonation and deprotonation of polypyrrole chain in aqueous solutions, Synth. Met. 45 (1991) 35–48.

[51] H.-S. Park, S.-J. Ko, J.-S. Park, J.Y. Kim, H.-K. Song, Redox-active charge carriers of conducting polymers as a tuner of conductivity and its potential window, Sci. Rep. 3 (2013) 2454.

[52] N. Sakmeche, S. Aeiyach, J.-J. Aaron, M. Jouini, J.C. Lacroix, P.-C. Lacaze, Improvement of the electrosynthesis and physicochemical properties of poly(3,4-ethylenedioxythiophene) using a sodium dodecyl sulfate micellar aqueous medium, Langmuir 15 (1999) 2566–2574.

[53] S. Berbec, S. Zoladek, A. Jablonska, B. Palys, Electrochemically reduced graphene oxide on gold nanoparticles modified with a polyoxomolybdate film. Highly sensitive non-enzymatic electrochemical detection of H2O2, Sens. Actuators B Chem. 258 (2018) 745–756.

[54] L. Setti, A. Fraleoni-Morgera, I. Mencarelli, A. Filippini, B. Ballarin, M. Di Biase, An HRP-based amperometric biosensor fabricated by thermal inkjet printing, Sens. Actuators B Chem. 126 (2007) 252–257.

[55] Y.H. Yun, B.K. Lee, J.S. Choi, H.B. Yoo, Y.S. Kim, K. Park, Y.W. Cho, A glucose sensor fabricated by piezoelectric inkjet printing of conducting polymer and bien-zymes, Anal. Sci. 27 (2011) 375–379.

[56] H.W. Siao, S.M. Chen, K.C. Lin, Electrochemical study of PEDOT-PSS-MDB-modified electrode and its electrocatalytic sensing of hydrogen peroxide, J. Solid State Electrochem. 15 (2011) 1121–1128.

[57] A.E.O. Makowski, B. Kowalewska, K. Miecznikowski, P.J. Kulesza, Hybrid bioelectrocatalyst for hydrogen peroxide reduction: immobilization of enzyme within organic-inorganic film of structured Prussian Blue and PEDOT, Bioelectrochemistry 71 (2007) 23–28.

[58] J. Xu, R. Peng, Q. Ran, Y. Xian, Y. Tian, L. Jin, A highly soluble poly(3,4-ethylenedioxythiophene)-poly(styrene sulfonic acid)/Au nanocomposite for horseradish peroxidase immobilization and biosensing, Talanta 82 (2010) 1511–1515.

[59] Y. Yao, Y. Wen, L. Zhang, J. Xu, Z. Wang, X. Duan, A Stable Sandwich-Type Hydrogen Peroxide Sensor Based on Immobilizing Horseradish Peroxidase to a Silver Nanoparticle Monolayer Supported by PEDOT:PSS-Nafion Composite Electrode, Int. J. Electrochem. Sc. 8 (2013) 9348–9359.

[60] L.A. Mercante, M.H.M. Facure, R.C. Sanfelice, F.L. Migliorini, L.H.C. Mattoso, D.S. Correa, One-pot preparation of PEDOT:PSS-reduced graphene decorated with Au nanoparticles for enzymatic electrochemical sensing of H2O2, Appl. Surf. Sci. 407 (2017) 162–170.

[61] L. Zhang, H. Cheng, H. Zhang, L. Qu, Direct electrochemistry and electrocatalysis of horseradish peroxidase immobilized in graphene oxide–Nafion nanocomposite film, Electrochim. Acta 65 (2012) 122–126.

[62] M. Li, S. Xu, M. Tang, L. Liu, F. Gao, Y. Wang, Direct electrochemistry of horseradish peroxidase on graphene-modified electrode for electrocatalytic reduction towards H2O2, Electrochim. Acta 56 (2011) 1144–1149.